Food Chemistry 402 (2023) 134271

Contents lists available at ScienceDirect

Food Chemistry

journal homepage: www.elsevier.com/locate/foodchem

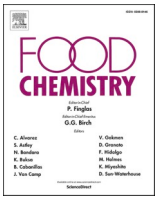

Docosahexaenoic acid in regio- and enantiopure triacylglycerols: Oxidative stability and influence of chiral antioxidant

Annelie Damerau [a], Eija Ahonen [a], Maaria Kortesniemi [a], Haraldur G. Gudmundsson [a,b], Baoru Yang [a], Gudmundur G. Haraldsson [b], Kaisa M. Linderborg [a,*]

[a] Food Sciences, Department of Life Technologies, University of Turku, 20014 Turun yliopisto, Turku, Finland
[b] Science Institute, University of Iceland, Dunhaga 3, 107, Reykjavik, Iceland

ARTICLE INFO

Keywords:
Autoxidation
DHA
Omega-3 fatty acid
TAG regioisomers
TAG enantiomers
Alpha-tocopherol

ABSTRACT

Docosahexaenoic acid (DHA) is essential for health but easily oxidized. Yet the influence of DHA's exact location (*sn*-1, *sn*-2, or *sn*-3) in triacylglycerols on oxidative stability is currently unknown. This is the first study comparing oxidative stability of DHA in regio- and enantiopure triacylglycerols with or without *RRR*-α-tocopherol. Headspace solid-phase micro-extraction with gas chromatography–mass spectrometry, liquid chromatography–mass spectrometry, and nuclear magnetic resonance spectroscopy were applied. DHA in *sn*-2 was the most stable with or without added *RRR*-α-tocopherol resulting in differences in hydroperoxide formation. Without antioxidant, stability of DHA in *sn*-1 and *sn*-3 was mainly similar, with slight tendency towards better stability in *sn*-3. With *RRR*-α-tocopherol higher stability in *sn*-1 compared to *sn*-3 was observed. This points to diastereomeric interactions between *RRR*-α-tocopherol and DHA in *sn*-1. These results are highly relevant for enzymatic restructuring processes of DHA-rich fish or microalgae oil concentrates aimed for food supplements or food fortification.

1. Introduction

Docosahexaenoic acid (DHA, C22:6) is a $n-3$ polyunsaturated fatty acid ($n-3$ PUFA), essential for human health. It is needed in normal development of the eyes and brains of infants, and linked with the increase of birth weight and gestational age. DHA is also associated with brain functions related to cognitive and emotional health, and it plays a role in inflammatory balance and in the stability of cardiovascular system (Hashimoto, Hossain, Al Mamun, Matsuzaki, & Arai, 2017). The primary dietary source of DHA is marine foods. In addition, DHA containing food supplements and foods enriched with DHA provide alternatives for consumers to increase their DHA intake.

DHA oxidizes easily and the oxidation products can be absorbed by the human body. Oxidation of DHA-containing triacylglycerols (DHA-TAGs), the most common lipid form in foods, yields a multitude of oxidation products, including oxo-fatty acids as regio- and stereoisomers. The oxo-fatty acids are biologically active and toxic, and thus of high physiological importance (Vieira, Zhang, & Decker, 2017). Carboxyethylpyrrole, one oxidation product of DHA, has been shown to form adducts with proteins and lipids, which again have been linked to inflammation-associated diseases (Yakubenko and Byzova, 2017). Therefore, studying oxidation of DHA containing TAGs is of importance for human health.

In TAGs DHA is located in the *sn*-1, *sn*-2 or *sn*-3 positions of the glycerol backbone. Recent research shows that the position in TAGs influences the bioavailability of DHA. DHA located in the *sn*-2 position is well absorbed by the intestinal mucosa and favorably used for synthesis of TAGs and phospholipids in the body (Jin, Jin, Wang, & Akoh, 2020). Better bioavailability of DHA in *sn*-2 position compared to *sn*-1 and *sn*-3 was also shown in our own study using enantiomerically pure DHA containing TAGs in a rat feeding trial (Linderborg et al. 2019). The influence of structural characteristics of TAGs on the oxidative stability of $n-3$ PUFAs has been studied only decades back by randomization of natural oils or synthetic TAGs, yet with contradictory results (Endo, Hoshizaki, & Fujimoto, 1997; Frankel, Selke, Neff, & Miyashita, 1992; Miyashita, Frankel, Neff, & Awl, 1990; Park, Terao, & Matsushita, 1983; Yamamoto, Imori, & Hara, 2014). No general oxidation behavior, e.g. for the degree of unsaturation of fatty acids could be described. A major obstacle for such studies has been the lack of regio- or stereopure model compounds suitable for these kinds of studies.

* Corresponding author.
E-mail address: kaisa.linderborg@utu.fi (K.M. Linderborg).

https://doi.org/10.1016/j.foodchem.2022.134271
Received 24 May 2022; Received in revised form 1 August 2022; Accepted 12 September 2022
Available online 15 September 2022

The only currently published study investigating the regio-isomeric effect on oxidative stability of DHA in TAGs using a regiopure TAG model found that DHA was more stable to oxidation when located at the *sn*-2 position in TAGs compared to *sn*-1 or *sn*-3 (Wijesundera et al., 2008). Their study was undertaken without addition of antioxidants. However, the oxidative stability of *sn*-1 vs *sn*-3 was not compared due to the lack of enantiopure TAGs. This study includes regiopure symmetrically structured ABA type TAGs and regio- and enantiopure asymmetrically structured AAB type TAGs. To the knowledge of the authors, this is the first oxidative study undertaken on enantiopure compounds. Further, the presented study researches also for first time the impact of chirality of DHA containing TAGs on the ability of a common chiral antioxidant, in this case *RRR*-α-tocopherol, to protect DHA against oxidation. This is of interest as it has been shown that stereoisomeric effects can influence oxidation kinetics (Danilack, Mulvihill, Klippenstein, & Goldsmith, 2021). All natural products rich in DHA and products fortified with DHA contain natural or added antioxidants. Therefore, studying lipid oxidation of DHA in TAGs also in the presence of antioxidants is of importance to determine the regio- and stereoisomeric effect in food products.

The hypothesis of this study was that the oxidative stability of DHA and *RRR*-α-tocopherol response are dependent on DHA location on the glycerol backbone in TAGs. Therefore, the main aim was to compare the oxidative stability of DHA in terminal *sn*-1 and *sn*-3 positions in TAGs considering the enantiomeric differences between them. Further, the *sn*-2 position was also compared to the terminal *sn*-1,3-positions in TAGs. The study also investigated whether the location at the enantiospecific *sn*-1 or *sn*-3 positions of the glycerol skeleton in enantiopure TAGs renders them higher or lower protection against oxidation in the presence of natural *RRR*-α-tocopherol, which is enantiopure. To enable this study predesigned regiopure structured TAGs of the ABA type and regio- and enantiopure TAGs of the AAB type were synthesized and oxidized under controlled conditions. Oxidation behavior was studied using modern gas chromatographic (GC) or liquid chromatographic (LC) methods with mass spectrometric (MS) detection and nuclear magnetic resonance (NMR) spectroscopy to allow direct analysis of lipid oxidation compounds at different stages of oxidation. Headspace solid-phase micro extraction (HS-SPME) was used for extraction of volatile secondary oxidation products combined with GC–MS.

2. Materials and methods

2.1. Sample materials

Regiopure symmetrically structured ABA-type DHA-TAG (*sn*-2; 2DT) and regio- and enantiopure asymmetrically structured (*S*)-AAB (*sn*-1; 1DT) and (*R*)-AAB (*sn*-3; 3DT) DHA-TAGs synthesized from pure palmitic acid (C16:0; A) and DHA (B) (Larodan, Solna, Sweden) (see synthesis 2.2) were studied with and without addition of natural *RRR*-α-tocopherol (Sigma–Aldrich, Buchs, Switzerland) extracted from vegetable oil. Concentration of *RRR*-α-tocopherol was determined spectrophotometrically at 292 nm according to Podda, Weber, Traber, and Packer (1996) with Evolution 300 BB UV–vis spectrophotometer (Thermo Scientific, Waltham, MA, USA). TAG samples were kept under argon for transport and stored at −80 °C until analysis.

2.2. Synthesis of regiopure and enantiopure triacylglycerols

Regiopure symmetrically structured ABA-type DHA-TAG and regio- and enantiopure asymmetrically structured AAB-type [(S)-AAB and (R)-AAB] DHA-TAGs (1DT and 3DT, respectively) were synthesized. A two-step chemoenzymatic approach was followed for the ABA-type TAG (Halldorsson, Magnusson, & Haraldsson, 2003; Magnusson, & Haraldsson, 2010). This was based on a highly regioselective immobilized *Candida antarctica* lipase (CAL-B from Novozymes in Denmark) to act exclusively at the 1,3-positions of glycerol in the first step to afford the 1,3-DAG key intermediate possessing pure palmitic acid. The pure DHA was incorporated into the remaining 2-position by use of EDCI as a coupling agent. The synthesis of the asymmetrically structured AAB-type DHA-TAGs was executed via a five-step chemoenzymatic route using enantiopure solketals as chiral precursors (Kristinsson & Haraldsson, 2008; Kristinsson, Linderborg, Kallio, & Haraldsson, 2014). This was based on the use of benzyl ether as a protective group, the CAL-B lipase to introduce palmitic acid into the glycerol backbone and EDCI as a coupling agent to incorporate DHA into the appropriate terminal *sn*-1 or *sn*-3 positions in the final step. The synthetic details have been reported recently (Kalpio et al., 2020). The chemical and regioisomeric purity of all products and intermediates was fully established by ^{1}H and ^{13}C NMR and IR spectroscopy and accurate mass spectrometry (HRMS) analyses as well as the enantiomeric purity of the DHA-TAG enantiomers by chiral-phase recycling HPLC.

2.3. Experimental setup for the oxidation trial

The experimental setup used in our previous study on oxidative stability, α-tocopherol response and oxidation pattern of DHA incorporated in triacylglycerols and as ethyl esters (Ahonen, Damerau, Suomela, Kortesniemi, & Linderborg 2022) was adapted for this study. All model TAGs (1DT, 2DT and 3DT) were dissolved into *n*-hexane (VWR, Gliwice, Poland) and volumes representing 20 mg of DHA-TAGs transferred into 10 mL amber SPME-vials under dim light conditions. *RRR*-α-Tocopherol diluted in *n*-hexane was added in volumes representing 28 μg (0.14% w/w) to half of the prepared samples. Samples with *RRR*-α-tocopherol addition are referred to as 1αDT, 2αDT, and 3αDT from here on. Samples were stored under nitrogen at –80 °C until the start of the oxidation trial. For the oxidation trial, the samples were evaporated to dryness using nitrogen flow and the headspace of vials was filled with compressed air to provide oxygen for the oxidation reaction. Samples were oxidized at 50 °C using a Hewlett Packard 6890 Series Plus G1530A GC oven (Wilmington, DE, USA), and analyzed with HS-SPME-GC–MS at different oxidation time points (incubation and extraction time was included in total oxidation time). Samples without *RRR*-α-tocopherol were oxidized for 30.6 h (time points at 0.6 h, 6.6 h, 12.6 h, 18.6 h, 24.6 h and 30.6 h) and samples with *RRR*-α-tocopherol for 54.6 h (time points at 0.6 h, 22.6 h, 34.6 h, 42.6 h, 48.6 h and 54.6 h). Oxidation time points were selected based on pre-tests analyzing volatile secondary oxidation products (VSOPs) (see 2.7). Immediately after the HS-SPME, the vial was cooled down to room temperature, and 1 mL chloroform from Sigma–Aldrich (St. Louis, MO, USA) added. After precooling at –20 °C for 20 min the headspace was gently filled with nitrogen and the sample moved to –80 °C for further analysis. In addition, for each TAG model a real zero sample was prepared, which was not subjected to any heating but otherwise handled the same way as the oxidation trial samples. Three replicates of each sample type (1DT, 2DT, 3DT, 1αDT, 2αDT, and 3αDT) were prepared for each time point.

2.4. Fatty acid content

The content of fatty acids was analyzed with GC with flame ionization detector (FID) as methyl esters. 1 mg of sample in chloroform was flushed to dryness with nitrogen after addition of 0.3 mg internal standard (triheptadecanoin from Larodan, Solna, Sweden) in chloroform (Honeywell International Inc., Riedel de Haën, Germany) and methylated using the methanolic hydrogen chloride method according to Christie and Han (2010). Acetyl chloride and methanol were obtained from Sigma-Aldrich (Steinheim, Germany). A Shimadzu GC-2030 equipped with an AOC-20i auto injector, an FID (Shimadzu Corporation, Kyoto, Japan) and DB-23 column (60 m × 0.25 mm × 0.25 μm; Agilent Technologies, J.W. Scientific, Santa Clara, CA, USA) was used. GC conditions: helium flow 1.4 mL/min; 130 °C held 1 min, 6.5 °C/min to 170 °C, 2.75 °C/min to 205 °C, held for 18 min, 30 °C/min to 230 °C and held for 2 min. The peaks were identified by using external

standards 37 Component FAME mix (Supelco, St. Louis, MO, USA) and GLC-490 (Nu-Check-Prep, Elysian, MN, USA) and quantified using internal standard.

2.5. *RRR*-α-Tocopherol concentration

For *RRR*-α-tocopherol analysis 2 mg of samples in chloroform were transferred to heptane (Honeywell/Riedel de Haën, Seelze, Germany). *RRR*-α-Tocopherol concentrations were analyzed using normal phase high performance LC with fluorescence detection (NP-HPLC-FLD) according to the method by Schwartz, Ollilainen, Piironen, and Lampi (2008). The analysis was preformed using a HPLC system consisting of Shimadzu Nexera LC-20AD XR pump, SIL-20AC autosampler (set to 4 °C), CTO-20AC prominence column oven (set to 30 °C) and RF-20A prominence fluorescence detector (Shimadzu Corp., Kyoto, Japan) and equipped with a Phenomenex Luna® 3 μm silica column (250 × 4.6 mm) (Phenomenex®, Torrance, CA, USA). *RRR*-α-Tocopherol was analyzed isocratically using a mobile phase mixture of 3% 1,4-dioxane (Sigma–Aldrich, Steinheim, Germany) and 97% heptane (v/v) at a flow rate of 2 mL/min. The excitation wavelength was 295 nm and the emission wavelength 325 nm. For quantification, α-tocopherol standard curve (5, 20, 50, 100, 150, 200, 250 μg/mL) was prepared in heptane from an α-tocopherol (>96%; Sigma–Aldrich, Buchs, Switzerland) stock solution with pre-determined concentration (Podda et al., 1996). LabSolutions 5.93 (Shimadzu Corporation, Kyoto, Japan) was used for data analysis.

2.6. Non-volatile oxidation products (HPLC-QTOF)

Hydroperoxides and other non-volatile oxidation products were analyzed in an untargeted manner by HPLC with a quadrupole/time-of-flight tandem mass spectrometer (QTOF), utilizing the method by Ahonen et al. (2022). Elute UHPLC and Bruker Impact II QTOF instruments from Bruker Daltonic (Bremen, Germany) and Macherey-Nagel (Düren, Germany) column Nucleodur C18 Isis (250 mm × 4.6 mm, 5 μm particle size) were used. The column oven was set to 30 °C and the autosampler cooler to 4 °C. 1 mg of sample in chloroform was further diluted 1:40 (v/v) in chloroform and 2 μL was injected. A binary solvent system was applied including acetonitrile and water from Fisher Scientific (Loughborough, UK), and formic acid from VWR (Leuven, Belgium) as solvent A (50/50/0.1, v/v/v), and 2-propanol from Honeywell/Riedel de Haën (Seelze, Germany), water, and formic acid as solvent B (100/0.1/0.1, v/v/v). 10 mM ammonium acetate from Sigma–Aldrich (Steinheim, Germany) was added to both solvents. In the LC gradient program, the proportion of solvent B was increased from the initial level of 40% to 70% in 3 min, to 95% in 22 min, kept for 7 min, dropped back to 40% in 0.5 min, and kept for 5 min. The total flow rate was 0.8 mL/min of which 0.23 mL/min was directed to MS. Electrospray ionization (ESI) was applied in positive mode. The capillary voltage was set to 4.5 kV and end plate offset set to 500 V. Nebulizer gas pressure, drying gas flow rate, and drying gas temperature were 1.5 bar, 4 L/min, and 350 °C, respectively. Auto MS/MS scanning mode from 60 to 2000 *m/z* was applied. Internal calibration was performed using sodium formate. Data was analyzed by Bruker Compass DataAnalysis 5.1 (Bruker Daltonic GmbH, Bremen, Germany) software. Extracted-ion chromatograms (EIC) were utilized for collecting the peak area data.

2.7. Volatile secondary oxidation products (HS-SPME-GC–MS)

VSOPs were determined by HS-SPME-GC–MS (Damerau et al., 2020) using Thermo Scientific GC–MS instrument (Trace 1300 GC, ISQ 7000 single quadrupole MS, TriPlus RSH autosampler; Waltham, MA, USA) with SPB®-624 capillary column (60 m × 0.25 mm × 1.4 μm, Supelco, Bellafonte, PA, USA). For HS-SPME 20 mg of sample (see 2.3) was incubated for 1 min and then extracted for 30 min at 50 °C using a DVB/CAR/PDMS 50/30 μm (Supelco, Bellafonte, PA, USA) fiber. The fiber was desorbed for 10 min at 240 °C in the injection port of the GC, which was operated in splitless mode. The GC operation conditions were the following: helium flow 1.4 mL/min; oven temperature 40 °C for 6 min, then increased by 5 °C/min to 200 °C and held at 200 °C for 10 min. The ionization energy of the MS was 70 eV and the scan range was from 40 to 300 amu. Compound identification was based on NIST MS Search library (version 2.4, National Institute of Standards and Technology, Gaithersburg, MD, USA.) and data of external standards analyzed in our previous study (Ahonen et al., 2022). Acquired data was analyzed using Chromeleon 7.2.9 Chromatography Data System (Thermo Fisher Scientific, Waltham, MA, USA) and is reported as peak areas.

2.8. NMR spectroscopy

Overall oxidative changes were analyzed by ^{1}H NMR in an untargeted manner. Regio-specific excitation was employed for hydroperoxides and aldehydes as major oxidation products from DHA. NMR analysis was done from selected time points (for 1DT, 2DT, 3DT: 12.6 and 18.6 h; and for 1αDT, 2αDT, 3αDT: 42.6 and 48.6 h). 10 mg of sample in chloroform was taken for analysis and the chloroform was evaporated under nitrogen flow. Afterwards, 200 μL of dry $CDCl_3$ (Merck, Darmstadt, Germany) / DMSO-d_6 (VWR, Leuven, Belgium) (5:1; v/v) was added according to Merkx, Hong, Ermacora, and van Duynhoven (2018), the sample was transferred into 3-mm NMR tube and stored at – 20 °C in a desiccator until analysis. Data was collected according to the method used by Ahonen et al. (2022), which was based on the method from Merkx et al. (2018). A 600 MHz Bruker AVANCE-III NMR spectrometer (Bruker BioSpin, Switzerland) equipped with a Prodigy TCI CryoProbe and a SampleJet robotic sample changer operated at 600.16 MHz (^{1}H) at 298 K was used to record spectra. Proton spectra (*zg30*) were collected with 32 scans, sweep width of 14 ppm, receiver gain of 32, acquisition time of 4 s, and recycle delay of 5 s. Selective gradient excitation (*selgpse*) was applied on regions δ 11.5–10.5 ppm and δ 10.0–9.0 ppm for hydroperoxides and aldehydes, respectively. Selective ^{1}H spectra were collected with 128 scans, 4 dummy scans, receiver gain of 32, acquisition time of 2.7 s, and relaxation time of 5 s. The length of the 180-degree shaped pulse was 1566.15 μs. TopSpin 4.0.6 (Bruker Biospin Corporation, Billerica, MA, USA) and Chenomx NMR Suite 8.6 (Chemomx Inc., Edmonton, AB, Canada) was used to process the NMR data.

2.9. Statistical analysis

Fatty acid ratio, *RRR*-α-tocopherol content, and peak area data of non-volatile and volatile oxidation products of DHA-TAGs were compared for each time point using one-way ANOVA and Tukey's HSD test in SPSS (IBM SPSS Statistics, version 27.0.1.0, IBM Corporation, New York, USA) (Supplementary table 1). Differences were considered statistically significant if p-value was below 0.05. Principal component analysis (PCA) was applied to binned (0.001 ppm) and manually integrated NMR data after Pareto-scaling and mean-centering using SIMCA® 16 (Sartorius Stedim Data Analytics AB, Umeå, Sweden).

3. Results and discussion

3.1. Fatty acid ratio and RRR-α-tocopherol content

Ratio of DHA to C16:0 in TAGs samples was used as one oxidation indicator as the content of C16:0 was expected to remain stable during oxidation, and DHA to be consumed. In the beginning of the oxidation trial all samples had a DHA to C16:0 wt ratio of approximately 0.61 (Fig. 1). The ratio of DHA to C16:0 in both 1DT and 3DT started to decrease at 12.6 h showing consumption of DHA. The ratio in 3DT decreased significantly slower at 12.6 and 18.6 h than in 1DT (Supplementary table 1), which indicated a higher oxidation rate for 1DT compared to 3DT. Ratio of DHA to C16:0 in 2DT was relatively stable during the oxidation period, only slightly decreasing at 30.6 h, which

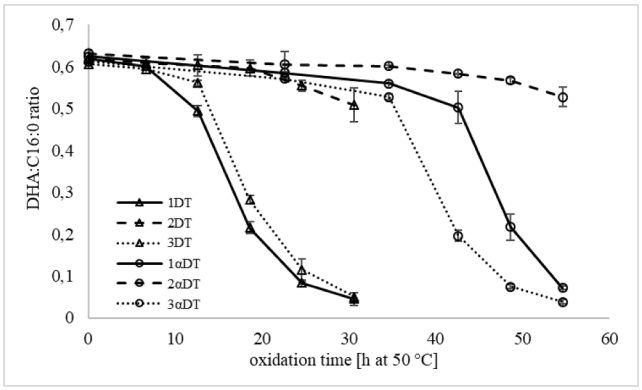

Fig. 1. Docosahexaenoic acid (DHA) to palmitic acid (C16:0) weight ratio development during 30.6 h or 54.6 h oxidation trial at 50 °C for docosahexaenoic acid (DHA) containing triacylglycerols (TAGs) without *RRR*-α-tocopherol and with DHA in *sn*-1 (1DT), *sn*-2 (2DT) and *sn*-3 (3DT) position, or with *RRR*-α-tocopherol and with DHA in *sn*-1 (1αDT), *sn*-2 (2αDT) and *sn*-3 (3αDT) position, respectively, (n = 3).

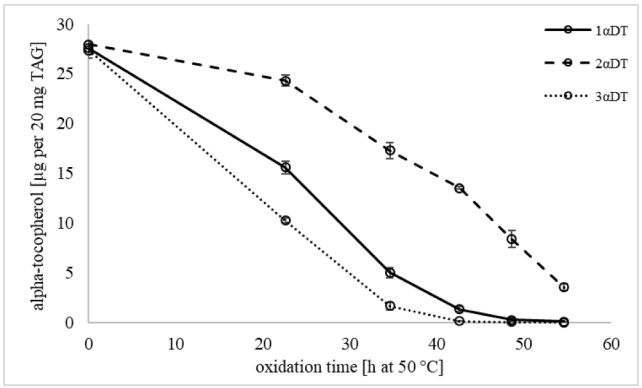

Fig. 2. *RRR*-α-Tocopherol concentration (µg/20 mg TAG) development during 54.6 h oxidation trial at 50 °C for docosahexaenoic acid (DHA) containing triacylglycerols (TAGs) with DHA in *sn*-1 (1αDT), *sn*-2 (2αDT) and *sn*-3 (3αDT) position (n = 3).

implied significantly higher oxidative stability of 2DT when compared to 1DT and 3DT. Wijesundera et al. (2008) used similar regiopure model TAGs containing DHA and C16:0 to study oxidative stability of DHA. They also reported significantly higher oxidative stability of DHA at *sn*-2 position compared to *sn*-1(3) according to DHA to 16:0 ratios. However, in their case the model TAGs oxidized faster although their oxidation trial was carried out at similar temperature as in this study. This is maybe related to differences in other conditions of the oxidation trial. E. g. they used oxygen in headspace during the oxidation trial, while in this study air was used to closer mimic the situation in foods. The higher oxygen pressure in the study of Wijesundera et al. (2008) compared to in this study could have accelerated autoxidation in their case.

The addition of antioxidant *RRR*-α-tocopherol significantly increased the oxidation stability of all TAG models as expected, increasing the DHA consumption time through oxidation. The initial DHA to C16:0 wt ratio in all models with *RRR*-α-tocopherol was similar as for the ones without addition (Fig. 1). The ratio in 2αDT was like in 2DT stable throughout the oxidation trial, only slightly decreasing in the end. The DHA to C16:0 ratios in 1αDT and 3αDT started to decrease at 34.6 h. The decrease was notably faster for 3αDT than for 1αDT until the last time point (Supplementary table 1). This was the opposite from what was seen without addition, where DHA in 1DT was less stable than in 3DT. Higher stability of DHA in *sn*-1 when compared to *sn*-3 position could indicate diastereomeric interactions between DHA in *sn*-1 position and *RRR*-α-tocopherol.

In the beginning of oxidation trial all TAG models contained similar amount of *RRR*-α-tocopherol (27.6 µg per 20 mg TAG, Fig. 2). Already, after 22.6 h the content dropped under half of the original content for 3αDT and at 54.6 h no *RRR*-α-tocopherol was detectable in 3αDT. In the case of 1αDT, the content of *RRR*-α-tocopherol decreased significantly slower than for 3αDT (Supplementary table 1) and at 54.6 h still 0.1 µg was found. 2αDT had the highest remaining content of *RRR*-α-tocopherol at 54.6 h with 3.5 µg and showed the shallowest slope in overall consumption (Fig. 2). Therefore, the *RRR*-α-tocopherol response showed comparable behavior to the DHA to C16:0 ratio (Fig. 1) during the oxidation trial with DHA being most stable in *sn*-2 followed by *sn*-1and *sn*-3 position.

3.2. Non-volatile oxidation products analyzed by UHPLC-QTOF

For the collection of quantitative peak area data for the non-volatile oxidation products, extracted ion chromatograms (EIC) of sodium $[M + 23]^+$ and $[M + 18]^+$ ammonium adduct ions were applied. Ammonium adduct ions were most abundant for the non-oxidized compound and sodium adduct ions for oxygen-containing molecules. Altogether 16 oxidation products were identified based on their fragmentation patterns (Table 1).

The most abundant fragment for the ammoniated non-oxidized 16:0/16:0/22:6 was the neutral loss of 22:6 (*m/z* 551.5), followed by the

Table 1
Compound mass (*m/z*), ammonium $[M + 18]^+$ and sodium $[M + 23]^+$ adduct masses (*m/z*), retention times (min) and the main fragments for identification (*m/z*, of the underlined adduct) in the order of lowering intensity for 16:0/16:0/22:6 and identified oxidation products analyzed by HPLC-QTOF.

Compound	*m/z*	$[M + 18]^+$	$[M + 23]^+$	RT	Main fragments
16:0/16:0/22:6	878.8	896.8	901.7	22.3	551.5 / 623.5 / 311.2 / 239.2
M + 16 Da	894.7	912.8	917.7	19.8	367.2 / 551.5 / 661.5 / 239.2
M + 14 Da	892.7	910.7	915.7	18.4	365.2 / 551.5 / 659.5 / 239.2
M + 2O	910.7	928.7	933.7	17.8	887.7 / 915.7 / 807.6 / 806.6 / 847.6
16:0/16:0/19:5; O2	870.7	888.7	893.7	16.3	551.5 / 597.5 / 579.4
16:0/16:0/6:1;O	680.5	698.6	703.5	15.3	551.5 / 425.3 / 313.3
M + 4O	942.7	960.7	965.7	15.1	415.2 / 551.5 / 893.7 / 847.6
16:0/16:0/6:1;O2 or 16:0/16:0/ 7:0;O	696.5	714.6	719.5	15.0	313.3 / 551.5 / 441.3
16:0/16:0/13:2; O3	808.6	826.7	831.6	14.8	551.5 / 221.1 / 313.3
16:0/16:0/18:5; O2	856.6	874.7	879.6	14.5	551.5 / 583.4 / 601.4 / 271.1
M + 6O	974.7	992.7	997.7	14.4	551.5 / 742.6 / 447.2
16:0/16:0/5:1;O2 or 16:0/16:0/6:0;O	682.5	700.6	705.5	14.2	427.3 / 551.5
16:0/16:0/12:3; O2	776.6	794.6	799.6	13.7	551.5 / 313.3 / 521.3 / 503.3
M + 7O	990.7	1008.7	1013.7	13.2	551.5 / 313.3 / 239.2
M + 8O	1006.7	1024.7	1029.7	13.0	551.5 / 313.3 / 239.2
M + 9O	1022.7	1040.7	1045.7	12.6	551.5 / 313.3 / 239.2
M + 10O	1038.7	1056.7	1061.7	12.4	551.5 / 313.3 / 239.2

neutral loss of 16:0 (*m/z* 623.5), 22:6 acyl chain (*m/z* 311.2), and 16:0 acyl chain (*m/z* 239.2). For the additions of 16 Da and 14 Da, the main fragments for the sodiated molecular ion were 22:6 + Na + 16/14 Da (*m/z* 367.2/365.2), loss of the oxidized acyl chain (*m/z* 551.5), and loss of 16:0 (*m/z* 661.5/659.5). The mass addition of 16 Da could be either an epoxide that has formed to the site of a double bond, or a hydroxide (Xia & Budge, 2017), and the mass addition of 14 Da could be a ketone or an epoxide, which has formed next to a double bond (Neff & Byrdwell, 1998). For the M + 14 Da, only the first peak eluting approximately at 18.0–19.4 min was integrated (Supplementary Fig. 1), as the latter could include fragments from M + 16 Da. The mass addition of two oxygens (+32 Da) to the non-oxidized compound includes monohydroperoxides as well as structures with two separate oxygens, e.g., epoxides and/or hydroxides. However, in the samples with the highest M + 2O intensities, the most abundant fragments for the total peak area contained *m/z* values corresponding to different

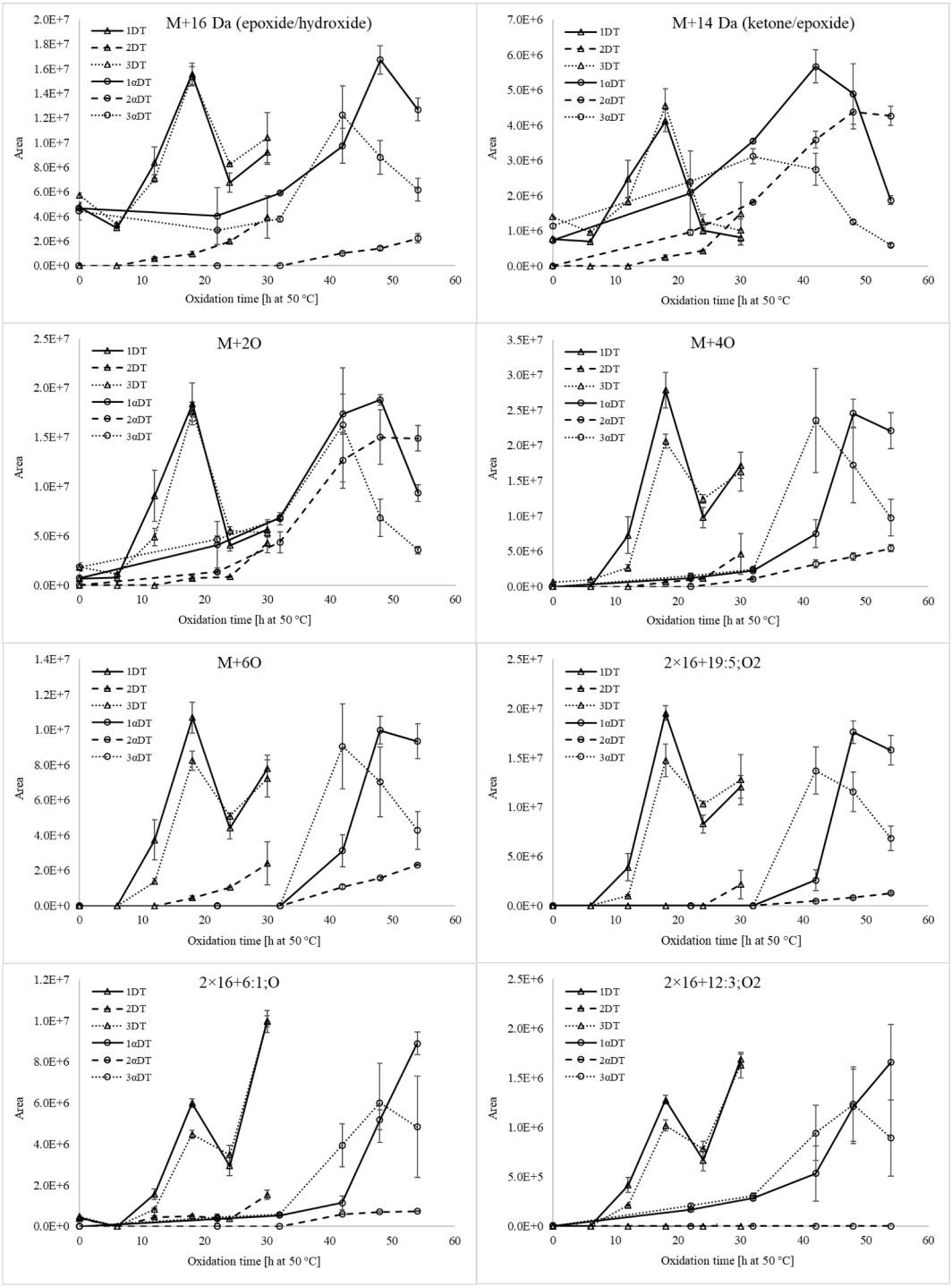

Fig. 3. Area development of oxidation products M + 16 Da, M + 14 Da, M + 2O, M + 4O, M + 6O, 2 × 16 + 19:5;O2, 2 × 16 + 6:1;O, and 2 × 16 + 12:3;O2 in the samples oxidized at 50 °C in the dark without (1DT:*sn*-1 DHA, 2DT:*sn*-2 DHA, and 3DT:*sn*-3 DHA) and with (1αDT:*sn*-1 DHA, 2αDT:*sn*-2 DHA, and 3αDT:*sn*-3 DHA) 0.14% *RRR*-α-tocopherol. Values are mean ± standard deviation of three replicates, except for 24 h oxidized 3DT, for which results are based on areas of two replicates.

monohydroperoxide isomers as deduced by the fragmentation patterns described by Ito, Mizuochi, Nakagawa, Kato, and Miyazawa (2015). The most abundant fragments corresponded to 20-OOH (−46 Da, *m/z* 887.7), and to loss of water (−18 Da, *m/z* 915.7). Also fragments for 14-OOH (−126 Da, *m/z* 807.6), 16-OOH (−127 Da, *m/z* 806.6), 17-OOH (−86 Da, *m/z* 847.6), 22:6 + Na + 2O (*m/z* 383.2) and loss of oxidized 22:6 (*m/z* 551.5) were among the ones with highest intensities. VanRollins and Murphy (1984) and, Lyberg, Fasoli, and Adlercreutz (2005) have investigated the distribution of DHA hydroperoxide isomers in free fatty acids and triacylglycerols during oxidation at room temperature. Results indicated the highest proportional abundancy of C20-OOH for DHA in free fatty acids (25–27%). For triacylglycerols with three DHAs, the isomer distribution was more equal, with the lowest prevalence for 13- and 14-OOH in the middle of the chain. Fragments for sodiated M + 4O and M + 6O contained loss of oxidized 22:6 (*m/z* 551.5), as well as the acyl chain with added oxygens, e.g., 22:6 + Na + 4O/6O (*m/z* 415.2/447.2). For M + 4O also fragments corresponding to 2 × 16 + 19:5;O2 (*m/z* 893.7) and 17-OOH (*m/z* 847.6) were detected. Altogether, additions of 2, 4, 6, 7, 8, 9, and 10 oxygens were perceived, with significantly lowering intensities along with the increasing number of oxygens. For the oxidation products with cleaved 22:6 chain, the identification was based on the possible structures deduced by the remaining chain mass after cleavage. Possible ether structures, as well as structures not originating from DHA, were excluded. Area development for M + 16 Da, M + 14 Da, M + 2O, M + 4O, M + 6O, 2 × 16 + 19:5;O2, 2 × 16 + 6:1;O, and 2 × 16 + 12:3;O2 in the samples with and without *RRR*-α-tocopherol is presented in Fig. 3, and extracted ion chromatograms for the same oxidation products in Supplementary Fig. 1.

In the samples without added *RRR*-α-tocopherol, 2DT was clearly distinguished from 1- and 3DT with lower formation rates for all oxidation products during the 30-h oxidation period. Lower formation rates of hydroperoxides based on peroxide value were also found for conjugated linolenic acid if primarily present in *sn*-2 position compared to *sn*-1(3) (Yamamoto et al., 2014). Wijesundera et al. (2008) also observed lower formation of monohydroperoxides for DHA in *sn*-2 than in *sn*-1(3). They described the differences in hydroperoxide formation as the main reason for improved stability of DHA in *sn*-2 compared to *sn*-1 (3). They attributed the differences in formation to interactions between acyl chains in the TAGs molecule having a protective impact on the acyl chain in *sn*-2 position as also suggested by Miyashita et al. (1990). In 1- and 3DT there was a 6-hour induction period before the fast formation of M + 16 Da, M + 14 Da and M + 2O started, while for M + 4O, M + 6O, and acyl chain cleavage products the induction period took 12 h. The maximum level was reached at 18 h, after which decomposition rate by reacting further became greater than the formation rate and the levels started to decrease. Especially for the short acyl chain cleavage products, there was a considerable second increase from 24 h to 30 h after the initial maximum at 18 h. The increase of M + 2O, M + 4O, M + 6O, and 2 × 16 + 19:5;O2 levels were slightly slower from 6 h to 12 h in 3DT when compared to 1DT, but the maximum was reached simultaneously at 18 h. Possibly a more frequent sampling might have revealed clearer differences in the induction period and maximum point between 1- and 3DT. Some accumulation of M + 16 Da and M + 14 Da was perceived already in the non-oxidized 1- and 3DT samples. Overall, it can be concluded that without added *RRR*-α-tocopherol DHA at the *sn*-2 position was clearly the most stable structure and between the *sn*-1 and *sn*-3 positions only minor difference in early formation rate was observed.

Also in the samples with 0.14% added *RRR*-α-tocopherol 2αDT was showing less oxidation product formation during the 54-hour oxidation period when compared to 1- and 3αDT. However, the formation of M + 14 Da and M + 2O was significant, although lower, also in the 2αDT samples. In the samples with *RRR*-α-tocopherol, also a difference between 1- and 3αDT was perceived. Improved stability of 1αDT when compared to 3αDT is shown in the area development of M + 16 Da, M + 2O, M + 4O, M + 6O, and acyl chain cleavage products as a longer induction period (42 vs 32 h) and/or later peak maximum (48 vs 42 h). In summary, the results showed superior stability of DHA at *sn*-2 position with 0.14% added *RRR*-α-tocopherol, and also DHA at *sn*-1 position could be distinguished from DHA at *sn*-3 position by its enhanced stability.

3.3. Volatile secondary oxidation products analyzed by HS-SPME-GC–MS

VSOPs are major group of secondary oxidation products and are especially important for sensory quality of DHA rich oils. They are mainly formed from scission of alkoxy radicals originating from hydroperoxides, cyclic peroxides and bicyclic endoperoxides. However, also breakdown products of secondary oxidation products are contributing to VSOPs (Frankel, Neff, & Selke, 1984). VSOPs identified in DHA containing TAGs are presented in Supplementary table 2. While all identified VSOPs were present in all samples regardless of enantiomer or addition of *RRR*-α-tocopherol their formation was different as expected based on differences seen for the formation of hydroperoxides (see 3.3). Acetaldehyde, propanal, acetic acid, 2-ethylfuran, 1-penten-3-one, 1-penten-3-ol, 2,4-heptadienal (*E,Z* and *E,E* combined) and 5-ethyl-2(5*H*)-furanone were selected as oxidation indicator compounds and their formation is shown in Fig. 4. They were selected based on formation pathway, use in previous studies as indicator compounds for DHA oxidation (Wijesundera et al. 2008) and, peak size and separation. Acetaldehyde among other compounds can be a product of further reactions of alkenals, polymers and malondialdehyde produced from lipid oxidation (Frankel, 1982; Vandemoortele, Heynderickx, Leloup, & De Meulenaer, 2021). Propanal can be formed as one breakdown product from 20-OOH, alkenals, polymers, hydroperoxy epidioxides and hydroperoxy bisepidioxides (Frankel, 1982; Frankel, Neff, & Selke, 1983). Acetic acid is a further oxidation product of acetaldehyde (Frankel, 1982). 2-Ethylfuran can be formed from either 2-hexenal, a product from scission of C16 or C17 alkoxy radicals (Frankel, Neff, & Selke, 1981), as described by Adams, Bouckaert, Van Lancker, De Meulenaer, and De Kimpe (2011) or from hydroperoxy epidioxides as found by Frankel et al. (1983). 1-Penten-3-one and 1-penten-3-ol are both reaction products of scission of C17 alkoxy radical, formed from 17-OOH through O—O cleavage (Hammer & Schieberle, 2013). 2,4-Heptadienal was found to be one further reaction product of 16-OOH, dihydroperoxides, hydroperoxy epidioxides, bicycloendoperoxides (Frankel et al., 1981, 1983, 1984). 5-Ethyl-2(5*H*)-furanone can be formed from 3-hexenal, a breakdown product from 16-/17-OOH (Frankel et al., 1981), via intra- or inter-molecular peracid oxidation as described by Buttery and Takeoka (2004).

A comparison of the formation curves for VSOPs with and without *RRR*-α-tocopherol revealed that autoxidation was further progressed in case without *RRR*-α-tocopherol than with in the observed time periods (Fig. 4). This could mainly be concluded based on whether decomposition and stabilization was reached in the end of the oxidation period. However, in both cases induction and propagation can be observed. Also minor differences in the total amounts of selected VSOPs were observed between oxidation trials without and with *RRR*-α-tocopherol. This difference could be caused by oxidation pathway alterations affecting the amount of formed VSOPs if *RRR*-α-tocopherol is present. However, the differences could also be caused by slightly different experimental conditions between trials and non-optimal time point selection to see maximum formation.

For the TAGs without addition of *RRR*-α-tocopherol an induction period of 6.6 h could be detected for all selected volatile indicator compounds except 2-ethylfuran (Fig. 4), which did not display any induction period. After the induction period a more rapid increase was noted. The induction period was most pronounced for 2DT. The overall formation of all selected volatile indicator compounds was lower for 2DT than for 1DT and 3DT throughout the oxidation trial with the exception of acetaldehyde and 2-ethylfuran in the end of oxidation period (Fig. 4). These exceptions are related to the decomposition of

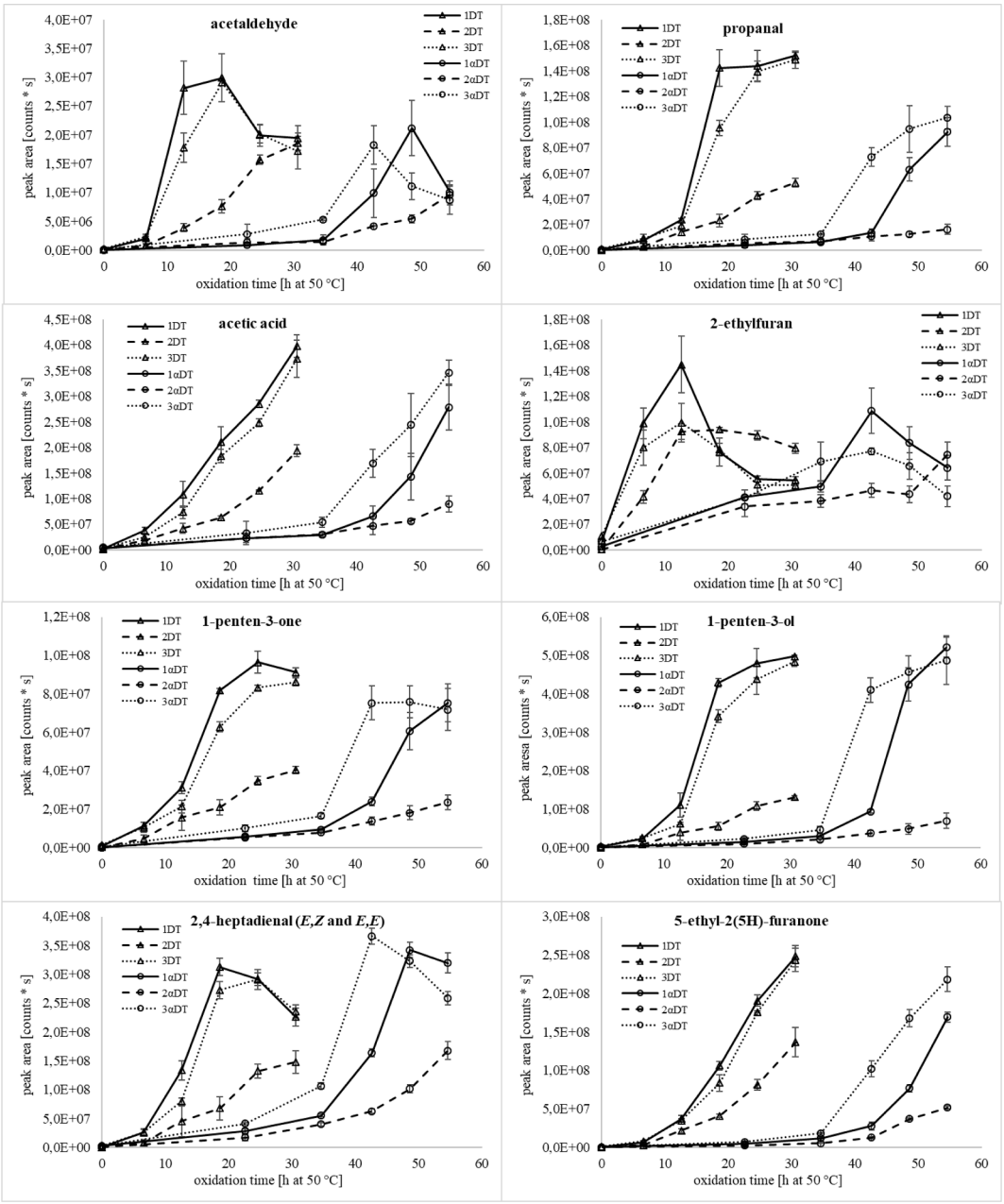

Fig. 4. Peak areas of acetaldehyde, propanal, acetic acid, 2-ethylfuran, 1-penten-3-one, 1-penten-3-ol, 2,4-heptadienal (*E,Z* and *E,E* combined) and ethyl-2(5*H*)-furanone during 30.6 h or 54.6 h oxidation trial at 50 °C for docosahexaenoic acid (DHA) containing triacylglycerols (TAGs) without *RRR*-α-tocopherol and with DHA in *sn*-1 (1DT), *sn*-2 (2DT) and *sn*-3 (3DT) position, or with *RRR*-α-tocopherol and with DHA in *sn*-1 (1αDT), *sn*-2 (2αDT) and *sn*-3 (3αDT) position, respectively, (n = 3).

acetaldehyde and 2-ethylfuran for 1DT and 3DT after 18.6 and 12.6 h, respectively. For 2DT a slight decrease was seen for 2-ethylfuran at 24.6 h. These differences in behavior can be explained by 2DT still being in an earlier stage of autoxidation than 1DT and 3DT, as already indicated in hydroperoxide formation. Similar formation of propanal and *E,E*-2,4-heptadienal for DHA in *sn*-2 vs *sn*-1(3) was seen by Wijesundera et al. (2008). They observed an induction period of 2 h, which was more noticeable for propanal than *E,E*-2,4-heptadienal similar as in this study. Further, they also detected a more clear induction period and overall lower formation for *sn*-2 than *sn*-1(3). However, the observed differences between *sn*-2 and *sn*-1(3) was less pronounced in their study than in this one and the samples also oxidized faster in their study than in ours. E.g. in the study by Wijesundera et al. (2008) *E,E*-2,4-heptadienal started to decompose after 7 h while in this study 2,4-heptadienal (*E,Z* and *E,E* combined) started only to decreases after 18.6 h. The dissimilarities could be related to differences in experimental set-up like oxygen pressure, or to differences in purity of model compounds. Wijesundera et al. (2008) used regiopure but not enantiopure models. The enantiopure models used in this study allowed also to study differences in VSOPs between *sn*-1 and *sn*-3. Overall the formation for selected volatile indicator compounds was similar for 1DT and 3DT with reaching similar levels at end of oxidation period (Fig. 4). However, slightly lower formation between 6.6 and 18.6 h could be observed for 3DT than 1DT, which was in line with previous observed minor difference in early formation rate of hydroperoxides between 1DT and 3DT.

With addition of *RRR*-α-tocopherol the induction period for the formation of VSOPs increased from 6.6 to 34.6 h except for 2-ethylfuran (Fig. 4), for which again no clear induction period could be seen. The

induction period was least pronounced for 3αDT. In case of acetaldehyde, acetic acid, 1-penten-3-one and 2,4-heptadienal (*E,Z* and *E,E* combined) it could also be argued that 3αDT had only an induction period of 22.6 h. However, the increase for all these VSOPs was more defined after 34.6 h. More time points between 22.6 and 34.6 h could be useful to determine the induction period more clearly in this case. No significant increase in propanal was observed until 42.6 h for 1αDT and until 54.6 h for 2αDT, respectively, displaying even longer induction periods (Fig. 4). Overall the formation of all selected VSOPs was lower for 2αDT than for 1αDT and 3αDT throughout the oxidation trial, which was similar as seen without the addition of *RRR*-α-tocopherol. The differences between *sn*-1 and *sn*-3 were more distinct with *RRR*-α-tocopherol than without (Supplementary table 1). Significantly higher formation for all selected VSOPs was detected from 22.6 to 42.6 h for 3αDT compared to 1αDT (Fig. 4, Supplementary table 1). In case of propanal, acetic acid and ethyl-2(5*H*)-furanone the formation was higher for 3αDT than 1αDT until the end of the oxidation period. For 3αDT acetaldehyde and 2,4-heptadienal (*E,Z* and *E,E* combined) started to decompose after 42.6 h, while for 1αDT a significant decrease in both volatiles was only noted after 48.6 h. This enforces the earlier

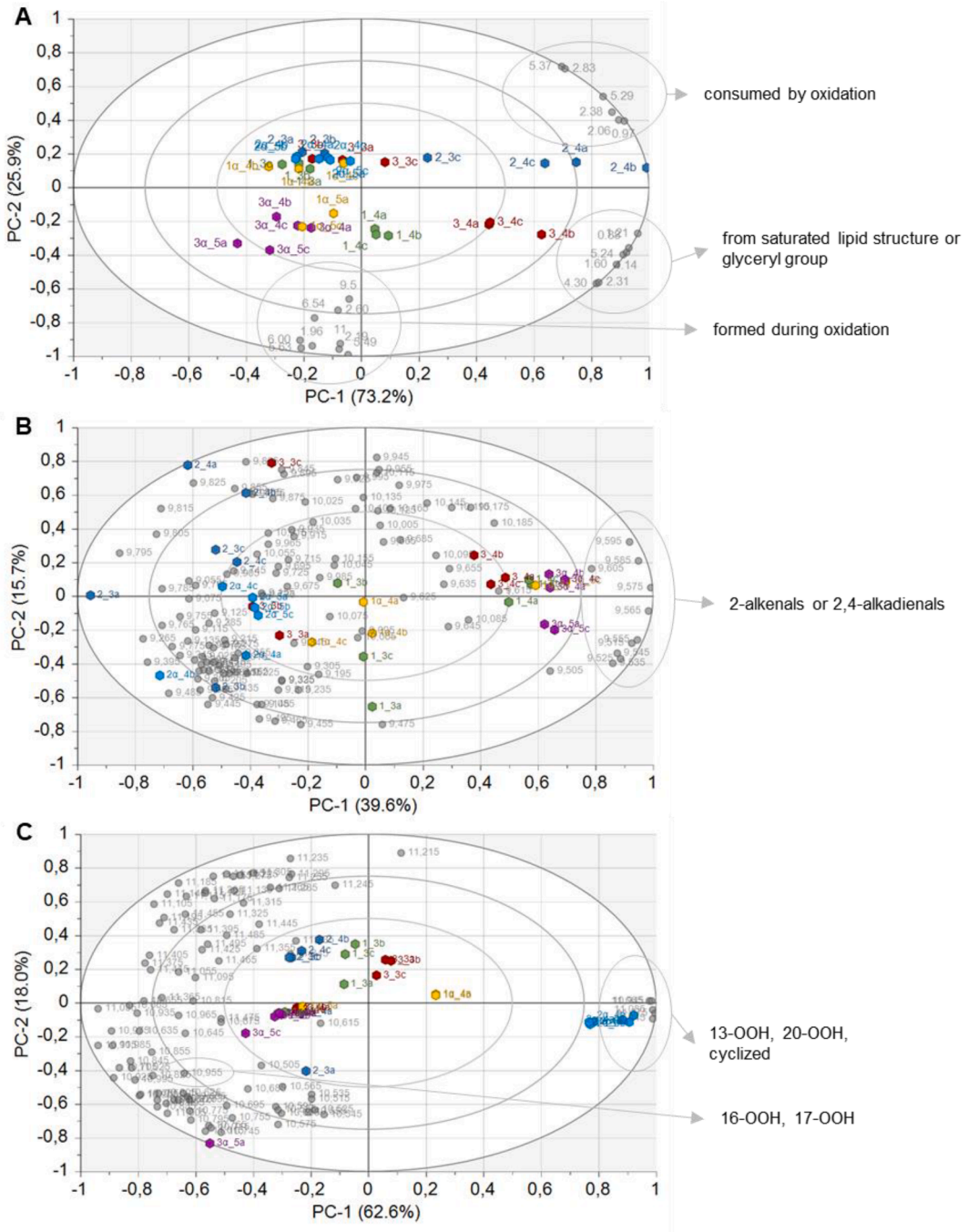

Fig. 5. PCA model for the manually integrated, Pareto-scaled and mean-centered NMR data of the aldehyde (10–9 ppm), hydroperoxide (11.5–10.5 ppm) and selected lipid structural regions as bi-plot (A) and PCA models for the binned, Pareto-scaled and mean-centered NMR data of selectively excited spectral regions 10–9 and 11.5–10.5 ppm for aldehydes (B) and hydroperoxides (C), respectively, as bi-plots. Observations are marked in different colors for each sample with sample codes: x_ty or xα_ty with x = 1, 2, 3 corresponding to *sn*-position of DHA, α indicating with or without *RRR*-α-tocopherol, t = time point (without α: 3 = 12.6 h and 4 = 18.6 h; with α: 4 = 42.6 h and 5 = 48.6 h, respectively) and y = replicate (a, b or c). Variables are marked in grey with chemical shift in ppm.

observation based on fatty acid ratio, remaining *RRR*-α-tocopherol content and non-volatile oxidation products that DHA is more oxidative stable in *sn*-1 than in *sn*-3 in the presence of *RRR*-α-tocopherol.

3.4. Overall oxidative change by NMR spectroscopy

^{1}H NMR was used to analyze the overall oxidative change, with a focus on hydroperoxides and aldehydes from selective time points, without *RRR*-α-tocopherol at 12.6 and 18.6 h and with *RRR*-α-tocopherol at 42.6 and 48.6 h, respectively. Time points were chosen based on observed formation of VSOPs. Compound identifications were made based on previous studies on DHA (Ahonen et al., 2022), linoleic acid (Wang et al. 2015) and edible oils (Martínez-Yusta, Goicoechea, & Guillén, 2014; Merkx et al., 2018), and are summarized in Supplementary table 3. The PCA models of ^{1}H NMR data are shown as bi-plots in Fig. 5. In bi-plot A the variables form three distinct clusters based on whether the molecule structure is consumed, formed or mostly untouched by oxidation. In the right upper corner, signals of diallylic methylene group (2.83 ppm), olefinic group (5.29 and 5.37 ppm), methyl group of DHA (0.97 ppm) and other signals related to the intact DHA molecule (2.06 and 2.38 ppm) could be found. These signals decreased over time indicating consumption through oxidation. Wang et al. (2015) also reported a decrease in corresponding signals for linoleic acid oxidation. They used the intensity of the diallylic methylene group to determine the amount intact linoleic acid as indicator of degree of oxidation. In the right lower corner, signals related to C16:0 like 0.88 ppm (methyl group) or 1.21 ppm (methylene group), and to the glyceryl group like 4.14 and 4.30 ppm are found (Fig. 5A). These structures are thought to stay intact during mild to moderate oxidation as investigated in this study. Signals from primary and secondary oxidation products like hydroperoxides (11.5–10.5 ppm) and aldehydes (10–9 ppm) are located in the left lower quarter of bi-plot A. Also signals of (*Z,E*)-conjugated double bonds associated with hydroperoxy group (5.49, 5.63, 6.00 and 6.54 ppm) could be found here. Interestingly, no signals related to (*E,E*)-conjugated double bonds associated with hydroperoxy group high enough to be clearly separated from the baseline could be found, when compared to the study by Wang et al. (2015) on linoleic acid oxidation. This can be explained by DHA providing an immediate internal H source through that the fatty acid chain bends back on itself, which favors formation of (*Z,E*)-conjugated double bonds in hydroperoxides compared to (*E,E*)-conjugated double bonds, which are in turn favored under H doner lacking conditions (Schaich, 2005).

Based on variable loadings in the bi-plot A (Fig. 5) it was concluded that the degree of oxidation is mainly explained along a diagonal from left upper corner to right lower corner. For all samples, except of 3αDT, the later of the two analyzed time points could be found lower and more on the right side than the earlier time point. This behavior was the least pronounced for all *sn*-2 samples, which are all found on the positive side of PC-2 and not associated with any signals related to oxidation compounds. This confirms the earlier findings using other analytical methods that *sn*-2 is more oxidatively stable than any of the other isomers. Wang et al. (2015) analyzed the effect of positional distribution of linoleic acid on oxidative stability using ^{1}H NMR. They also came to conclusion that *sn*-2 position provided higher resistance to oxidation than *sn*-1(3).

Comparing *sn*-1 vs *sn*-3, all the earlier time points, except for 3αDT, could be found on the positive side of PC-2, while the later time points are located on negative side of PC-2 closer to the signals of oxidation products (Fig. 5A). 1DT is more associated with oxidation compounds, while 3DT is more associated with signals related to saturated lipid structures and glyceryl group, which indicated slightly higher oxidative stability for 3DT compared to 1DT. In general, samples without *RRR*-α-tocopherol are further located on positive side of PC-1 than the ones with *RRR*-α-tocopherol. This can be explained by the samples at the time points chosen without *RRR*-α-tocopherol being less oxidized overall than the ones with *RRR*-α-tocopherol and therefore they associated more with the right side signal clusters. This is also confirmed by the VSOPs data for the corresponding time points (Fig. 4). Further, hydroperoxide stabilization by *RRR*-α-tocopherol may also play a role here as was seen in the formation of non-volatile oxidation products. 3αDT was associated more with oxidation compounds than 1αDT already at the earlier time point. This clearly indicates a higher oxidative stability for *sn*-1 compared to *sn*-3 if *RRR*-α-tocopherol is present.

Bi-plot B (Fig. 5) showed excited spectral region 10–9 ppm related to signals from the aldehyde group. The highest intensity was found for signals related to 2-alkenals and 2,4-alkadienals, which are main aldehydes formed from oxidation of DHA (Frankel, 1982). These signals could be found on positive side of PC-1 one. Samples having strongest association with these signals were 3αDT (both time points), 1αDT (later time point), 1DT (later time point) and 3DT (later time point) in this order. In case of 2DT and 2αDT, all samples were found on negative side of PC-1. In general, bi-plot B confirms behavior seen in bi-plot A towards oxidative stability. Signals related to excited spectral region 11.5–10.5 ppm are shown in Fig. 5C. These signals are related to hydroperoxy group. Identifications of specific hydroperoxides was difficult but some observations could be made. Signals of 16-OOH and 17-OOH, which are among the most commonly formed hydroperoxides from DHA (Frankel et al., 1981, 1983, 1984), are found in left lower corner of bi-plot C. The association with these signals corresponded with the state of oxidation seen earlier. However, some outliers were observed mainly-one replicate of 2DT at 12.6 h, which grouped far away from the other replicates. One other interesting observation was that all replicates regardless of time point of 2αDT grouped together on the positive side of PC-1 associated with 13-OOH, 20-OOH and some cyclized hydroperoxides (Fig. 5C). This might be related to significant formation of M + 14 Da and M + 2O seen for 2αDT compared to 2DT, which might be related to some stabilization effect of *RRR*-α-tocopherol. Overall, ^{1}H NMR data confirmed the previous findings made by LC-MS and HS-SPME-GC–MS. Interestingly, differences in oxidative stability between *sn*-1 and *sn*-3 without *RRR*-α-tocopherol could be more distinguished using ^{1}H NMR. Based on this, without antioxidants present the oxidative stability of DHA was slightly better in *sn*-3 position than in *sn*-1.

4. Conclusion

DHA was most stable in *sn*-2 position in TAGs regardless of the presence of *RRR*-α-tocopherol in bulk oil. This confirmed earlier findings by Wijesundera et al., 2008 using regiopure model TAGs without antioxidant addition. The difference in oxidation rate observed for TAG regioisomers may be attributed to the interaction of acyl chains within the same TAG molecule and possible steric hindrance for hydroperoxide formation. For the first time, differences in oxidative stability of DHA located in *sn*-1 and *sn*-3 position of entiopure TAGs were studied. Without the presence of *RRR*-α-tocopherols, oxidative stability of DHA in *sn*-1 and *sn*-3 position was mainly similar. However, there was a slight tendency towards better stability at *sn*-3. Most interestingly, in the presence of *RRR*-α-tocopherol, DHA at the *sn*-1 was more stable compared to that at the *sn*-3 position. This could be caused by diastereomeric interactions between DHA in *sn*-1 position and *RRR*-α-tocopherol increasing the protective effect of *RRR*-α-tocopherol.

The results of this study are highly relevant for DHA rich fish or micro algae oil concentrates to be used as food supplements or in food fortification. By enzymatic restructuring processes, used after upper concentration step, the position of $n-3$ PUFAs in TAGs can be influenced (Jin et al., 2020). This could be used to improve oxidative stability if enzymes with right regio- and enantiospecificity are chosen. The findings of this study are based on bulk oil models and further research is needed to see if these findings translate to other foods systems. There is already some evidence for emulsion systems closer resembling real foods. Shen and Wijesundera (2009) showed that their results for bulk oil in regards to stability of regiopure model TAGs could also translate to emulsions.

CRediT authorship contribution statement

Annelie Damerau: Conceptualization, Methodology, Formal analysis, Investigation, Writing – original draft, Writing – review & editing, Visualization, Supervision, Funding acquisition. **Eija Ahonen:** Methodology, Formal analysis, Investigation, Writing – original draft, Writing – review & editing, Visualization, Funding acquisition. **Maaria Kortesniemi:** Methodology, Formal analysis, Investigation, Writing – original draft, Writing – review & editing, Visualization, Supervision. **Haraldur G. Gudmundsson:** Methodology, Writing – review & editing. **Baoru Yang:** Resources, Writing – review & editing. **Gudmundur G. Haraldsson:** Conceptualization, Methodology, Resources, Writing – review & editing, Supervision, Funding acquisition. **Kaisa M. Linderborg:** Conceptualization, Methodology, Resources, Writing – original draft, Writing – review & editing, Supervision, Project administration, Funding acquisition.

Declaration of Competing Interest

The authors declare that they have no known competing financial interests or personal relationships that could have appeared to influence the work reported in this paper.

Data availability

Data will be made available on request.

Acknowledgements

The authors would like to thank Dr. Jukka-Pekka Suomela for the guidance of using UHPLC -QTOF and Linda Intonen for assistance with part of the practical work related to fatty acid analysis. Personal financial grant to Annelie Damerau from the Finnish Cultural Foundation is acknowledged. Further, personal financial grants to Eija Ahonen from Niemi Foundation, the Finnish Cultural Foundation and the Finnish Food Research Foundation are acknowledged. This work entity was carried out as part of the Academy of Finland funded project “Omics of oxidation – Solutions for better quality of docosahexaenoic and eicosapentaenoic acids” (grant number 315274, PI Kaisa M. Linderborg).

Appendix A. Supplementary data

Supplementary data to this article can be found online at https://doi.org/10.1016/j.foodchem.2022.134271.

References

Adams, A., Bouckaert, C., Van Lancker, F., De Meulenaer, B., & De Kimpe, N. (2011). Amino acid catalysis of 2-alkylfuran formation from lipid oxidation-derived α, β-unsaturated aldehydes. *Journal of Agricultural and Food Chemistry, 59*(20), 11058–11062. https://doi.org/10.1021/jf202448v

Ahonen, E., Damerau, A., Suomela, J.-K., Kortesniemi, M., & Linderborg, K. M. (2022). Oxidative stability, oxidation pattern and α-tocopherol response of docosahexaenoic acid (DHA, 22:6*n*–3)-containing triacylglycerols and ethyl esters. *Food Chemistry, 387*, Article 132882. https://doi.org/10.1016/j.foodchem.2022.132882

Buttery, R. G., & Takeoka, G. R. (2004). Some unusual minor volatile components of tomato. *Journal of Agricultural and Food Chemistry, 52*(20), 6264–6266. https://doi.org/10.1021/jf040176a

Christie, W. W., & Han, X. (2010). Lipid analysis. Isolation, Separation, Identification and Lipidomic Analysis. (4th ed.). Bridgwater. England: The Oily Press, (chapter 7).

Damerau, A., Ahonen, E., Kortesniemi, M., Puganen, A., Tarvainen, M., & Linderborg, K. M. (2020). Evaluation of the composition and oxidative status of omega-3 fatty acid supplements on the Finnish market using NMR and SPME-GC–MS in comparison with conventional methods. *Food Chemistry, 330*, Article 127194. https://doi.org/10.1016/j.foodchem.2020.127194

Danilack, A. D., Mulvihill, C. R., Klippenstein, S. J., & Goldsmith, C. F. (2021). Diastereomers and low-temperature oxidation. *The Journal of Physical Chemistry A, 125*(36), 8064–8073. https://doi.org/10.1021/acs.jpca.1c05635

Endo, Y., Hoshizaki, S., & Fujimoto, K. (1997). Oxidation of synthetic triacylglycerols containing eicosapentaenoic and docosahexaenoic acids: Effect of oxidation system and triacylglycerol structure. *Journal of the American Oil Chemists' Society, 74*, 1041–1045. https://doi.org/10.1007/s11746-997-0022-3

Frankel, E. N. (1982). Volatile lipid oxidation products. *Progress in Lipid Research, 22*(1), 1–33. https://doi.org/10.1016/0163-7827(83)90002-4

Frankel, E. N., Neff, W. E., & Selke, E. (1981). Analysis of autoxidized fats by gas chromatography-mass spectrometry: VII. Volatile thermal decomposition products of pure hydroperoxides from autoxidized and photosensitized oxidized methyl oleate, linoleate and linolenate. *Lipids, 16*(5), 279–285. https://doi.org/10.1007/bf02534950

Frankel, E. N., Neff, W. E., & Selke, E. (1983). Analysis of autoxidized fats by gas chromatography-mass spectrometry: VIII. Volatile thermal decomposition products of hydroperoxy cyclic peroxides. *Lipids, 18*(5), 353–357. https://doi.org/10.1007/bf02537231

Frankel, E. N., Neff, W. E., & Selke, E. (1984). Analysis of autoxidized fats by gas chromatography-mass spectrometry. IX. Homolytic vs. Heterolytic cleavage of primary and secondary oxidation products. *Lipids, 19*(10), 790–800. https://doi.org/10.1007/bf02534473

Frankel, E. N., Selke, E., Neff, W. E., & Miyashita, K. (1992). Autoxidation of polyunsaturated triacylglycerols. IV. Volatile decomposition products from triacylglycerols containing linoleate and linolenate. *Lipids, 27*, 442–446. https://doi.org/10.1007/BF02536386

Halldorsson, A., Magnusson, C. D., & Haraldsson, G. G. (2003). Chemoenzymatic synthesis of structured triacylglycerols by highly regioselective acylation. *Tetrahedron, 59*(46), 9101–9109. https://doi.org/10.1016/j.tet.2003.09.059

Hammer, M., & Schieberle, P. (2013). Model studies on the key aroma compounds formed by an oxidative degradation of ω-3 fatty acids initiated by either copper (II) ions or lipoxygenase. *Journal of Agricultural and Food Chemistry, 61*(46), 10891–10900. https://doi.org/10.1021/jf403827p

Hashimoto, M., Hossain, S., Al Mamun, A., Matsuzaki, K., & Arai, H. (2017). Docosahexaenoic acid: One molecule diverse functions. *Critical Reviews in Biotechnology, 37*, 579–597. https://doi.org/10.1080/07388551.2016.1207153

Ito, J., Mizuochi, S., Nakagawa, K., Kato, S., & Miyazawa, T. (2015). Tandem mass spectrometry analysis of linoleic and arachidonic acid hydroperoxides via promotion of alkali metal adduct formation. *Analytical Chemistry, 87*(9), 4980–4987. https://doi.org/10.1021/acs.analchem.5b00851

Jin, J., Jin, Q., Wang, X., & Akoh, C. C. (2020). High *sn*-2 docosahexaenoic acid lipids for brain benefits, and their enzymatic syntheses: A review. *Engineering, 6*(4), 424–431. https://doi.org/10.1016/j.eng.2020.02.009

Kalpio, M., Magnússon, J. D., Gudmundsson, H. G., Linderborg, K. M., Kallio, H., Haraldsson, G. G., & Yang, B. (2020). Synthesis and enantiospecific analysis of enantiostructured triacylglycerols containing n-3 polyunsaturated fatty acids. *Chemistry and Physics of Lipids., 231*, Article 104937. https://doi.org/10.1016/j.chemphyslip.2020.104937

Kristinsson, B., & Haraldsson, G. G. (2008). Chemoenzymatic synthesis of enantiopure structured triacylglycerols. *Synlett, 14*, 2178–2182. https://doi.org/10.1055/s-2008-1077981

Kristinsson, B., Linderborg, K. M., Kallio, H., & Haraldsson, G. G. (2014). Synthesis of eantiopure structured triacylglycerols. *Tetrahedron Asymmetry, 25*(2), 25–132. https://doi.org/10.1016/j.tetasy.2013.11.015

Linderborg, K. M., Kulkarni, A., Zhao, A., Zhang, J., Kallio, H., Magnusson, J. D., … Yang, B. (2019). Bioavailability of docosahexaenoic acid 22:6(n-3) from enantiopure triacylglycerols and their regioisomeric counterpart in rats. *Food Chemistry, 283*, 381–389. https://doi.org/10.1016/j.foodchem.2018.12.130

Lyberg, A. M., Fasoli, E., & Adlercreutz, P. (2005). Monitoring the oxidation of docosahexaenoic acid in lipids. *Lipids, 40*(9), 969–979. https://doi.org/10.1007/s11745-005-1458-1

Magnusson, C. D., & Haraldsson, G. G. (2010). Chemoenzymatic synthesis of symmetrically structured triacylglycerols possessing short-chain fatty acids. *Tetrahedron, 66*(14), 2728–2731. https://doi.org/10.1016/j.tet.2010.01.110

Martínez-Yusta, A., Goicoechea, E., & Guillén, M. D. (2014). A Review of thermo-oxidative degradation of food lipids studied by ^{1}H NMR spectroscopy: Influence of degradative conditions and food lipid nature. *Comprehensive Reviews in Food Science and Food Safety, 13*(5), 838–859. https://doi.org/10.1111/1541-4337.12090

Merkx, D. W. H., Hong, G. T. S., Ermacora, A., & van Duynhoven, J. P. M. (2018). Rapid quantitative profiling of lipid oxidation products in a food emulsion by ^{1}H NMR. *Analytical Chemistry, 90*(7), 4863–4870. https://doi.org/10.1021/acs.analchem.8b00380

Miyashita, K., Frankel, E. N., Neff, W. E., & Awl, R. A. (1990). Autoxidation of polyunsaturated triacylglycerols. III. Synthetic triacylglycerols containing linoleate and linolenate. *Lipids, 25*, 48–53. https://doi.org/10.1007/BF02562427

Neff, W. E., & Byrdwell, W. (1998). Characterization of model triacylglycerol (triolein, trilinolein and trilinolenin) autoxidation products via high-performance liquid chromatography coupled with atmospheric pressure chemical ionization mass spectrometry. *Journal of Chromatography A, 818*(2), 169–186. https://doi.org/10.1016/s0021-9673(98)00553-6

Park, D. K., Terao, J., & Matsushita, S. (1983). Influence of the positions of unsaturated acyl groups in glycerides on autoxidation. *Agricultural and Biological Chemistry, 47*(10), 2251–2255. https://doi.org/10.1080/00021369.1983.10865949

Podda, M., Weber, C., Traber, M. G., & Packer, L. (1996). Simultaneous determination of tissue tocopherols, tocotrienols, ubiquinols, and ubiquinones. *Journal of Lipid Research, 37*(4), 893–901. https://doi.org/10.1016/s0022-2275(20)37587-8

Schaich, K. M. (2005). Lipid oxidation: Theoretical aspects. In F. Shahidi (Ed.), *Bailey's industrial oil and fat products* (6th ed., pp. 269–355). New York: John Wiley & Sons Inc.

Schwartz, H., Ollilainen, V., Piironen, V., & Lampi, A.-M. (2008). Tocopherol, tocotrienol and plant sterol contents of vegetable oils and industrial fats. *Journal of Food Composition and Analysis, 21*(2), 152–161. https://doi.org/10.1016/j.jfca.2007.07.012

Shen, Z., & Wijesundera, C. (2009). Effects of docosahexaenoic acid positional distribution on the oxidative stability of model triacylglycerol in water emulsion. *Journal of Food Lipids, 16*, 62–71. https://doi.org/10.1111/j.1745-4522.2009.01132.x

Vandemoortele, A., Heynderickx, P. M., Leloup, L., & De Meulenaer, B. (2021). Kinetic modeling of malondialdehyde reactivity in oil to simulate actual malondialdehyde formation upon lipid oxidation. *Food Research International, 140*, Article 110063. https://doi.org/10.1016/j.foodres.2020.110063

VanRollins, M., & Murphy, R. C. (1984). Autooxidation of docosahexaenoic acid: Analysis of ten isomers of hydroxydocosahexaenoate. *Journal of Lipid Research, 25* (5), 507–517. https://doi.org/10.1016/s0022-2275(20)37802-0

Vieira, S. A., Zhang, G., & Decker, E. A. (2017). Biological implications of lipid oxidation products. *Journal of the American Oil Chemists' Society, 94*, 339–351. https://doi.org/10.1007/s11746-017-2958-2

Wang, X.-Y., Yang, D., Gan, L.-J., Zhang, H., Shin, J.-A., Lee, Y.-H., … Lee, K.-T. (2015). Effect of positional distribution of linoleic acid on oxidative stability of triacylglycerol molecules determined by ^{1}H NMR. *Journal of the American Oil Chemists' Society, 92*, 157–165. https://doi.org/10.1007/s11746-015-2590-y

Wijesundera, C., Ceccato, C., Watkins, P., Fagan, P., Fraser, B., Thientong, N., & Perlmutter, P. (2008). Docosahexaenoic acid is more stable to oxidation when located at the *sn*-2 position of triacylglycerol compared to *sn*-1(3). *Journal of the American Oil Chemists' Society, 85*, 543–548. https://doi.org/10.1007/s11746-008-1224-z

Xia, W., & Budge, S. M. (2017). Techniques for the analysis of minor lipid oxidation products derived from triacylglycerols: Epoxides, alcohols, and ketones. *Comprehensive Reviews in Food Science and Food Safety, 16*(4), 735–758. https://doi.org/10.1111/1541-4337.12276

Yakubenko, V. P., & Byzova, T. V. (2017). Biological and pathophysiological roles of end-products of DHA oxidation. *Biochimica et Biophysica Acta (BBA) - Molecular and Cell Biology of Lipids, 1862*(4), 407–415. https://doi.org/10.1016/j.bbalip.2016.09.022

Yamamoto, Y., Imori, Y., & Hara, S. (2014). Oxidation behavior of triacylglycerol containing conjugated linolenic acids in *sn*-1(3) or *sn*-2 position. *Journal of Oleo Science, 63*(1), 31–37. https://doi.org/10.5650/jos.ess13129